



SHORT COMMUNICATION

Rtp801 Suppression of Epithelial mTORC1 Augments Endotoxin-Induced Lung Inflammation

Aaron M. Nadon, Mario J. Perez, Daniel Hernandez-Saavedra, Lynelle P. Smith, Yimu Yang, Linda A. Sanders, Aneta Gandjeva, Jacob Chabon, Daniel E. Koyanagi, Brian B. Graham, Rubin M. Tuder, and Eric P. Schmidt

From the Program in Translational Lung Research, Division of Pulmonary Sciences and Critical Care Medicine, Department of Medicine, University of Colorado School of Medicine, Aurora, Colorado

Accepted for publication
June 2, 2014.

Address correspondence to Eric P. Schmidt, M.D., University of Colorado School of Medicine, Research Complex 2, Mail Stop C272, 12700 E 19th Ave, Aurora, CO 80045. E-mail: eric.schmidt@ucdenver.edu.

The mechanistic target of rapamycin (mTOR) is a central regulator of cellular responses to environmental stress. mTOR (and its primary complex mTORC1) is, therefore, ideally positioned to regulate lung inflammatory responses to an environmental insult, a function directly relevant to disease states such as the acute respiratory distress syndrome. Our previous work in cigarette smoke-induced emphysema identified a novel protective role of pulmonary mTORC1 signaling. However, studies of the impact of mTORC1 on the development of acute lung injury are conflicting. We hypothesized that Rtp801, an endogenous inhibitor of mTORC1, which is predominantly expressed in alveolar type II epithelial cells, is activated during endotoxin-induced lung injury and functions to suppress anti-inflammatory epithelial mTORC1 responses. We administered intratracheal lipopolysaccharide to wild-type mice and observed a significant increase in lung Rtp801 mRNA. In lipopolysaccharide-treated *Rtp801*^{-/-} mice, epithelial mTORC1 activation significantly increased and was associated with an attenuation of lung inflammation. We reversed the anti-inflammatory phenotype of *Rtp801*^{-/-} mice with the mTORC1 inhibitor, rapamycin, reassuring against mTORC1-independent effects of Rtp801. We confirmed the proinflammatory effects of Rtp801 by generating a transgenic Rtp801 overexpressing mouse, which displayed augmented inflammatory responses to intratracheal endotoxin. These data suggest that epithelial mTORC1 activity plays a protective role against lung injury, and its inhibition by Rtp801 exacerbates alveolar injury caused by endotoxin. (*Am J Pathol* 2014, 184: 2382–2389; <http://dx.doi.org/10.1016/j.ajpath.2014.06.002>)

In the past decade, increasing scientific attention has been devoted to the role of the mechanistic (formerly mammalian) target of rapamycin (mTOR) in the maintenance of cellular homeostasis.¹ mTOR signaling occurs via two well-defined, evolutionarily conserved complexes named mTORC1 and mTORC2. mTORC1, the best characterized of the mTOR complexes, primarily functions in the transduction of cell growth signals. mTORC1 signaling is activated during states of nutrient (eg, amino acids, lipids, and glucose) availability and growth factor stimulation. Activated mTORC1, in turn, activates downstream targets such as ribosomal S6 kinase, promoting protein synthesis and cell growth.² Accordingly, nutrient deprivation and environmental stress attenuate mTORC1 signaling, mediated by several upstream pathways that converge on the mTORC1 inhibitory complex TSC-1 (hamartin)/TSC-2 (tuberin).

Acute respiratory distress syndrome (ARDS) is a common and morbid critical illness characterized by the diffuse and rapid onset of neutrophilic pulmonary inflammation in response to either a direct (eg, pneumonia) or an indirect (eg, nonpulmonary sepsis) pulmonary insult.³ Several known modifiers of mTOR signaling have been implicated in the pathophysiological characteristics of ARDS, such as oxidative stress and localized hypoxia (both of which inhibit mTORC1^{4,5}), as well as local inflammatory cytokine expression (associated with mTORC1 activation⁶). Interestingly, published reports conflict regarding the impact of

Supported by NIH grants K08 HL105538 (E.P.S.), R01 ES016285 (R.M.T.), and T32 HL007171 (D.H.-S.).

Disclosures: The ptetSplice801 flag plasmid was provided by Quark Pharmaceuticals (Fremont, CA).

mTORC1 signaling in ARDS.^{7–10} Because these conflicting studies were on the basis of the systemic use of the pharmacological mTORC1 inhibitor rapamycin, their discrepant results could reflect varied effects of mTORC1 across the complex multicellular microenvironment of the injured alveolus. Furthermore, few studies have addressed the endogenous regulation of mTORC1 signaling during the onset and progression of lung injury.

In mice, cigarette smoke inhalation increases pulmonary expression of Rtp801 (alias *Redd1* or *Ddit4*), an endogenous activator of TSC-2, and, consequently, inhibitor of mTORC1.⁴ Within the lungs, Rtp801 is primarily localized to type II alveolar epithelial cells.⁴ Rtp801-mediated inhibition of epithelial mTORC1 activity during cigarette smoke inhalation augments alveolar injury, contributing to emphysema formation. Concordantly, RTP801 expression is increased in lung samples collected from human subjects with emphysema.⁴ These findings indicate that Rtp801/mTORC1 signaling functions to sense environmental stressors, integrating epithelial injury responses within the lungs.

Given that bacterial-originated lipopolysaccharide (LPS) might be recognized as an environmental threat, we hypothesized that Rtp801 expression would increase in a mouse LPS model of ARDS, with the ensuing suppression of epithelial mTORC1 consequently augmenting lung inflammation. We investigated this hypothesis by using a model of direct (intratracheal LPS) lung injury in wild-type (WT) mice and *Rtp801*-knockout (*Rtp801*^{−/−}) mice. These investigations were complemented by the development of transgenic mice that overexpressed Rtp801, to determine whether mTORC1 inhibition would lower the threshold for LPS-induced lung injury. Neutrophilic inflammation was correlated to cell-specific measures of mTORC1 activity, demonstrating the complex cellular heterogeneity of mTORC1 activity within the injured lung.

Materials and Methods

Reagents

LPS (*Escherichia coli* 055:B5), rapamycin, and dimethyl sulfoxide (DMSO) were purchased from Sigma (St. Louis, MO).

Animals

All mouse experiments were approved by the Institutional Animal Care and Use Committee of the University of Colorado (Aurora, CO). The care and handling of animals were in accord with NIH guidelines for ethical animal treatment. Animals were maintained in standard housing at the University of Colorado Anschutz Medical Center with ad libitum access to food and water. Animals of identical age and housing (ie, littermates) were randomly assigned to experimental or control groups.

We generated 8- to 12-week-old *Rtp801*^{−/−} male mice (C57BL/6 x 129SvEv) and WT littermates, as previously described.⁴ To generate Rtp801-overexpressing mice, rat

Ddit4 gene (encoding Rtp801) was first cloned and sequenced. The p_{tet}Splice801 flag plasmid provided by Quark Pharmaceuticals (Fremont, CA) was amplified in *E. coli*, and the EcoRI-restricted product (780 Kb) was used as a template to clone the *Ddit4* gene. The p_{tet}Splice801 flag EcoRI fragment was PCR amplified using the forward primer JBO-5 (5'-CGGATCCGCCACCATGGAGCAAAAGCTGATTTCTGAGGAGGATCTGCCTAGCCTCTGGGATCG-3'), which added a BamHI restriction site, a myc flag, and a Kozak sequence to the Rtp801 coding sequence. The reverse primer JBO-2 (5'-GAAGCTTCAACACTCTTCAATGAGCA-3') was used to amplify the *Rtp801* coding sequence, including a HindIII restriction site. The 731-bp PCR product was purified and cloned using the TA-TOPO cloning system (Invitrogen, Carlsbad, CA), following the conditions described by the manufacturer. Colonies were screened via restriction with EcoRI. Clones with inserts of the correct size were sequenced with Ampli Taq DNA polymerase FS (Applied Biosystems, Foster City, CA) with the dRhodamine terminator cycle-sequencing ready-reaction kit (Applied Biosystems) at the DNA sequencing and analysis core facility of the University of Colorado Cancer Center and analyzed with the PC/GENE software version 6.7 (IntelliGenetics, Mountain View, CA). The selected TOPO myc-RTP-801 plasmid was amplified in *E. coli* and restricted with BamHI and HindIII. The released fragments were cloned into the BamHI and HindIII of the pTRE2 vector (Clontech Laboratories, Mountain View, CA), following the conditions described by the manufacturer. Colonies were screened via restriction with BamHI and HindIII enzymes. Clones with inserts of the correct size were sequenced as described above. The pTRE2-myc-RTP-801 plasmid was amplified in *E. coli*, and the XhoI/SapI-restricted purified product (2.4 Kb) was used for injection in an egg of the C57BL6 mouse strain in the Transgenic Mouse Core of the University of Cincinnati (Cincinnati, OH) to produce the Tg-TRE-RTP-801 mouse.

Mouse Model of Lung Injury

Briefly, we anesthetized mice with i.p. ketamine and xylazine and suspended them by their incisors in a prone position at a 45-degree angle. We visualized the vocal cords using a small-animal laryngoscope (Penn-Century, Wyndmoor, PA) and instilled LPS (2 mg/kg in PBS; total volume, 50 μ L) or 50 μ L PBS for control into the trachea using a MicroSprayer aerosolizer (Penn-Century). At 4 or 24 hours after tracheal instillation, we re-anesthetized the mice with i.p. ketamine and xylazine. Once anesthetized, mice were sacrificed via exsanguination and bilateral thoracotomies. We performed bronchoalveolar lavage (BAL) with three 1-mL aliquots of ice-cold PBS and/or harvested lungs for analysis, as previously described.⁴

Rtp801-TRE Experiments

Ten days before acute lung injury experiments, we induced expression of the *Rtp801* transgene by the intratracheal

administration of 1×10^9 plaque-forming units (in 50 μ L PBS) of the tet-off tTA-adenovirus [or green fluorescent protein (GFP)—adenovirus as control] to Tg-TRE-RTP-801 mice anesthetized with ketamine/xylazine. After completion of the experimental protocol (24 hours after LPS), expression of the *Rtp801* transgene was confirmed via mRNA quantitative real-time PCR (qPCR) and protein immunofluorescence, as described below. Concurrent suppression of mTORC1 signaling was confirmed by immunofluorescent identification of the downstream mTORC1 target phosphorylated ribosomal S6, as described below.

Rapamycin Reversal of *Rtp801* Knockout Phenotype

As previously described,⁴ we treated WT mice and *Rtp801*-knockout mice with either 1.8% DMSO in PBS (200 μ L, administered via i.p. injection) or rapamycin (1 mg/kg; diluted in 200 μ L 1.8% DMSO in PBS) daily for 7 days before treatment with intratracheal LPS (2 mg/kg). Twenty-four hours after LPS, we performed BAL and harvested organs for analysis, as described above.

Assessment of Pulmonary Inflammation

We performed BAL differential counts, as previously described.⁴ Briefly, we determined the total BAL fluid cell count using a Bright-Line Hemacytometer (Hausser Scientific, Horsham, PA). We calculated neutrophil differentials using cytopspins from aliquots of BAL fluid after staining using the Hema 3 manual staining protocol (Fisher Scientific, Waltham, MA).

Assessment of Pulmonary Histological Characteristics

We performed histological analysis on paraffin-embedded, formalin-fixed sections (4 μ m thick), as previously described.⁴ An automated tissue stainer (Shandon Varistain Gemini ES; Thermo Scientific, Waltham, MA) performed hematoxylin and eosin staining. Slides were randomized and coded. A pathologist (R.M.T.), masked to slide identity, quantified lung injury using an American Thoracic Society—endorsed scoring system.¹¹ This score, ranging from 0 (no injury) to 1 (severe injury), is on the basis of a weighted average of neutrophils in the alveolar space, neutrophils in the interstitial space, hyaline membranes, proteinaceous airspace debris, and alveolar septal thickening.¹¹ The mean linear intercept was determined in saline-treated WT and *RTP801*^{-/-} mice (Metamorph, Molecular Devices, Sunnyvale, CA), as previously described.⁴ In addition, the alveolar surface volume (S/V) ratio was determined stereologically in the left lung. Images consisted of alveolated left lung, excluding areas that contained large airways or vessels. The lowest magnification that allowed proper resolution was 10 \times . The grid consisted of 21 line segments for determination of alveolar septal intercepts (indicative of alveolar surface). Lung volume was estimated by point count using a

42-point grid, and positive counts referred to points that fell in lung tissue (septa, vessels, airways, and airspace). The S/V was determined by the following formula:

$$S/V = \frac{2 * \sum I}{L/P * \sum PL}; \quad (1)$$

where $\sum I$ represents the sum of alveolar septal intercepts across line probe; $\sum PL$: sum of points falling within the lung; and L/P: the ratio of line probe length/total point probes.

The images were processed by Metamorph digital processing, and a macro operation was developed that superimposed the sampling line/point grid to binary-processed images; positive events were then counted per image and summed to provide the total number of events per lung.

Immunofluorescence

We performed immunofluorescence, including colocalization experiments, on paraffin-embedded, formalin-fixed sections (4 μ m thick) of agarose inflated lungs, as previously described.¹² Primary antibodies included rabbit polyclonal antibody to phospho-S6 ribosomal protein—Ser235/236 (1:300, number 2211; Cell Signaling, Danvers, MA), goat polyclonal antibody to surfactant protein C (SPC; 1:100, sc-7705; Santa Cruz Biotechnology, Santa Cruz, CA), goat polyclonal antibody to Redd-1 (ie, *Rtp801*; 1:100, sc-46034; Santa Cruz Biotechnology), rat monoclonal antibody to mouse Mac-3 (1:50, M3/84; BD Pharmingen, San Jose, CA), and rat monoclonal antibody to mouse Ly-6B.2 (1:100, MCA771G; AbD Serotec, Raleigh, NC). Isotype antibodies served as negative controls: rabbit IgG (1:200, I-1000; Vector Laboratories, Burlingame, CA), goat IgG (1:200, I-5000; Vector Laboratories), and rat IgG (1:200, I-4000; Vector Laboratories). We performed image quantification using Metamorph, as previously described.¹³

Protein and mRNA Expression

After completion of the experimental protocol (4 or 24 hours after LPS), we harvested lungs for protein or mRNA analysis. Western blot analyses were completed as previously described.¹² Primary antibodies included the following: polyclonal rabbit antibody to phospho-S6 ribosomal protein—Ser235/236 (1:20,000, number 2211; Cell Signaling), polyclonal rabbit antibody to S6 ribosomal protein (1:20,000, number 2217; Cell Signaling), and polyclonal rabbit antibody to β -actin (1:40,000, number 4967; Cell Signaling).

Total RNA was extracted from lung homogenates by using the RNeasy kit (Qiagen, Valencia, CA). RNA concentration was determined by spectrophotometry. The expression of *Rtp801* in the transgenic samples after doxycycline induction was assessed by RT-qPCR using the primers TgTRETRTP forward (5'-CCATGGAGCAAAAGCTGATT-3') and TgTRETRTP reverse (5'-ACTGTTGCTGCTGTCCAGG-3')

under the following conditions: an aliquot of 1 μ g of total RNA (without DNase treatment) was reverse transcribed with the iScript Reverse Transcription Supermix (Bio-Rad Laboratories, Hercules, CA) in 20 μ L of total volume, according to the manufacturer's instructions. Samples were then stored at -20°C .

Real-time PCR was performed using the 7300 Real Time PCR System (Applied Biosystems) with SYBR Green PCR Master Mix (Applied Biosystems), as follows: 2 μ L of the appropriate dilution of the cDNA sample plus 18 μ L of a premade mixture containing 0.5 μ L 10 $\mu\text{mol/L}$ TgTRERTP forward primer, 0.5 μ L 10 $\mu\text{mol/L}$ TgTRERTP reverse primer, 10 μ L 2 \times SYBER Green PCR Master Mix (HS SYBR Green qPCR kit), and 7.0 μ L H_2O . The cycling parameters were as follows: stage 1, 50°C for 2 minutes;

stage 2, 95°C for 10 minutes; stage 3 ($\times 40$ cycles), 95°C for 15 seconds and 60°C for 1 minute; and stage 4 (dissociation), 95°C for 15 seconds, 60°C for 30 seconds, and 95°C for 15 seconds.

Relative gene expression (in comparison to both experimental controls and the housekeeping gene, cyclophilin A) was determined by the comparative C_T method ($2^{-\Delta\Delta C_T}$). In studies demonstrating absence of Rtp801 in knock-out mice, expression was determined only in comparison to cyclophilin A ($2^{-\Delta C_T}$). Primers for cyclophilin A were m_rCycl74 forward (5'-CGACTGTGGACAGCTCTA-AT-3') and m_rCycl74 reverse (5'-CCTGAGCTACA-GAAGGAATG-3'). qPCR was similarly performed for heme oxygenase 1 [HO-1; forward (5'-GGTCAGGTGTCCAGAG-AAGG-3'); reverse (5'-CTTCCAGGGCCGTGTAGATA-3')]

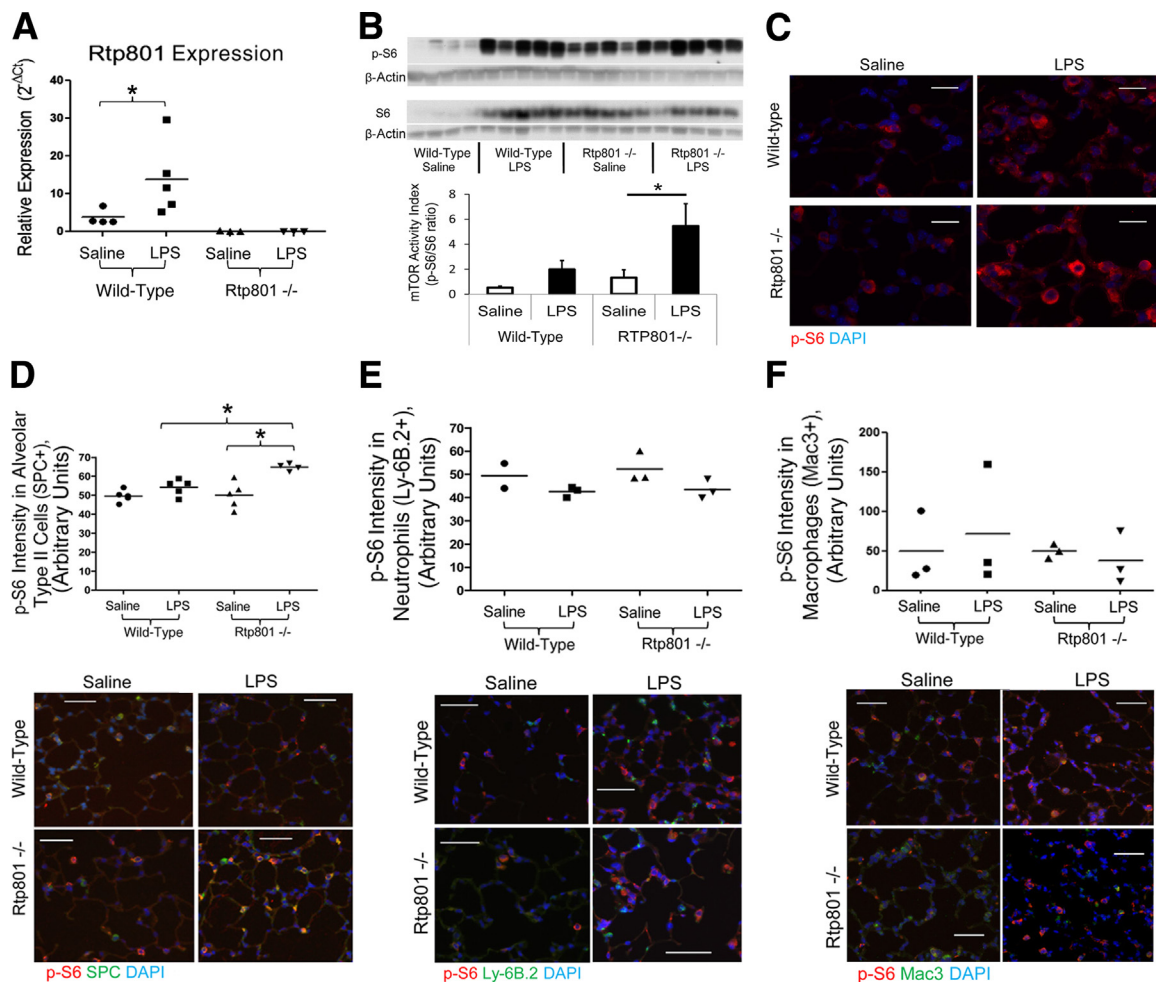


Figure 1 Rtp801 suppresses LPS activation of epithelial mTORC1. **A:** Four hours after 2 mg/kg intratracheal LPS, pulmonary expression of Rtp801 is significantly increased in WT mice, as assessed by qPCR. Rtp801 expression is absent in *Rtp801*^{-/-} mice. Expression is quantified as $2^{-\Delta C_T}$, normalized to the housekeeping gene cyclophilin A. Pulmonary mTORC1 activity (assessed by the relative phosphorylation of the mTORC1 target ribosomal S6, p-S6) increases nonsignificantly 4 hours after 2 mg/kg intratracheal LPS, as assessed by Western blot analysis of lung homogenates (**B**) and lung immunofluorescence (**C**). In the absence of Rtp801, LPS significantly increases pulmonary mTORC1 activity, demonstrating that Rtp801 induction functions to suppress LPS activation of pulmonary mTORC1. Immunofluorescent colocalization demonstrates that loss of Rtp801 augments mTORC1 signaling (p-S6) within alveolar type II epithelial cells (SPC positive, **D**) 4 hours after 2 mg/kg intratracheal LPS. No increase in p-S6 is noted within neutrophils (**E**) or macrophages (**F**). Red, p-S6; blue, DAPI; green, SPC (**D**), Ly-6B.2 (neutrophil marker, **E**), or Mac3 (macrophage marker, **F**); yellow, colocalization. * $P < 0.05$. $n = 3$ to 5 per group, except WT saline Ly-6B.2 ($n = 2$). Scale bars: 10 μm (**C**); 50 μm (**D–F**).

and with a TaqMan predesigned assay for tumor necrosis factor- α (TNF- α ; number 4331182; Applied Biosystems).

Statistical Analysis

Data are expressed as either scatter plots (accompanied by means) or bar graphs with SEM. We used a Student's two-tailed *t*-test when comparing two groups. Multiple comparisons were performed by one-way analysis of variance with Bonferroni's post hoc testing. Differences were statistically significant if $P \leq 0.05$. We performed all calculations using Prism version 5 (GraphPad, La Jolla, CA).

Results

LPS-Induced Lung Inflammation Is Exacerbated by Rtp801 Suppression of mTORC1

Intratracheal administration of LPS was associated with a rapid (4-hour) increase in pulmonary Rtp801 transcript expression (Figure 1A). WT animals demonstrated a nonsignificant trend toward increased pulmonary mTORC1 activity after LPS, as assessed by increased phosphorylation of ribosomal S6, a downstream target of mTORC1/S6K

(Figure 1, B and C). In the absence of Rtp801, LPS induced a substantial and statistically significant increase in mTORC1 activity (Figure 1, B and C), demonstrating that Rtp801 suppresses the pulmonary mTORC1 response to intratracheal LPS injury.

The impact of Rtp801 on mTOR signaling was most apparent within alveolar type II cells (Figure 1D), reflecting our previous observations that pulmonary Rtp801 was primarily localized to the alveolar epithelium.⁴ Consistent with this epithelial specificity, mTORC1 activity in pulmonary neutrophils (Figure 1E) and macrophages (Figure 1F) did not increase after intratracheal LPS and was not influenced by the absence of Rtp801.

Rtp801 Influences Pulmonary Inflammation via Regulation of mTORC1 Signaling

We sought to determine whether alteration of epithelial mTORC1 signaling (as measured 4 hours after intratracheal LPS) (Figure 1) affected the later development of neutrophilic pulmonary inflammation. In accordance with our previous findings,⁴ there were no baseline differences in lung morphometry findings between WT and *Rtp801*^{-/-} mice, with similar mean linear intercepts (28.1 ± 1.5 versus 27.0 ± 0.55

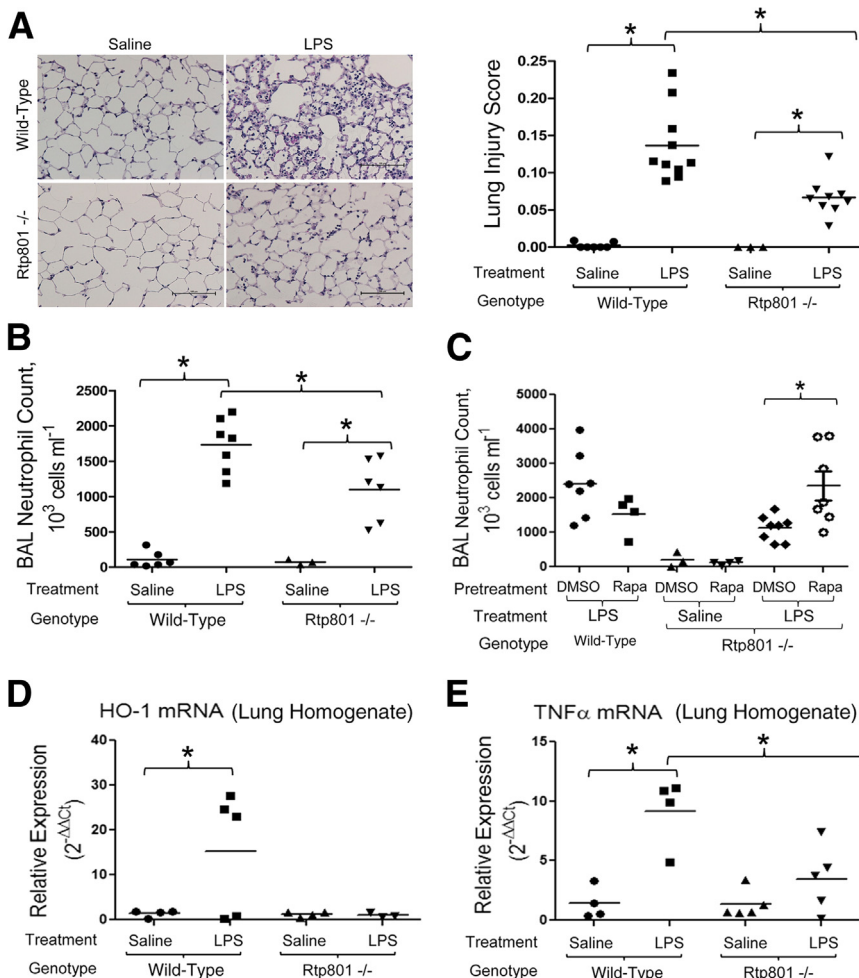


Figure 2 Rtp801 suppression of mTORC1 augments lung inflammation after LPS. Twenty-four hours after 2 mg/kg intratracheal LPS, significant pulmonary inflammation is apparent in lung histological features (hematoxylin and eosin, as quantified by a lung injury score ranging in severity from 0 to 1) (A) and BAL (B). Inflammation is significantly attenuated in *Rtp801*^{-/-} mice (A and B), demonstrating that epithelial mTORC1 activity functions to suppress pulmonary inflammation after intratracheal injury. C: The anti-inflammatory phenotype of *Rtp801*^{-/-} mice is lost after pretreatment with the mTORC1 inhibitor, rapamycin (Rapa; 1 mg/kg administered i.p. daily for 7 days before LPS), confirming that pulmonary mTORC1 activity opposes neutrophilic inflammation after intratracheal LPS. DMSO served as diluent control. Lung homogenate qPCR for HO-1 (D) and TNF- α (E) in WT or *Rtp801*^{-/-} mice 24 hours after intratracheal saline or LPS. Expression is quantified as $2^{-\Delta\Delta Ct}$, normalized to both the housekeeping gene cyclophilin A and intratracheal saline controls. * $P < 0.05$ (B–E). $n = 3$ to 10 per group (A and B); $n = 3$ to 9 per group (C); $n = 3$ to 4 per group (D and E). Scale bar = 100 μ m (A).

μm) and S/V ratios ($0.01 \pm 0.003 \mu\text{m}^{-1}$ versus $0.01 \pm 0.0001 \mu\text{m}^{-1}$), respectively ($n = 4$ to 6 per group). Pulmonary inflammation 24 hours after intratracheal LPS was attenuated by loss of Rtp801, as demonstrated by a dramatic attenuation of neutrophilic lung infiltration (Figure 2A). This protective effect was confirmed by an attenuation of alveolar neutrophilia in BAL fluid (Figure 2B). The anti-inflammatory phenotype of *Rtp801*^{-/-} mice was reversed by pretreatment with the mTORC1 inhibitor, rapamycin (Figure 2C), demonstrating that the effect of Rtp801 loss was directly consequent to augmented mTORC1 signaling. Interestingly, rapamycin pretreatment had a trend ($P = 0.18$) toward a paradoxically anti-inflammatory effect in LPS-treated WT mice, consistent with our previous findings.⁴

We sought to determine the mechanism underlying the anti-inflammatory phenotype of *Rtp801*^{-/-} mice. There were no differences in TUNEL staining (data not shown) between WT and *Rtp801*^{-/-} mice 24 hours after intratracheal LPS, suggesting that loss of *Rtp801* does not affect endotoxin-induced alveolar cell apoptosis. However, *Rtp801*^{-/-} mice demonstrated suppression of HO-1 (Figure 2D), a marker of (and potentially contributor to) oxidative stress.^{14,15} Similarly, *Rtp801*^{-/-} mice demonstrated suppression of TNF- α expression (Figure 2E) 24 hours after intratracheal LPS, suggesting that Rtp801-regulated mTORC1 activity influences the proinflammatory alveolar microenvironment.

Given the anti-inflammatory impact of loss of Rtp801, we anticipated that Rtp801 overexpression would augment LPS-

induced pulmonary inflammation. We inhibited pulmonary epithelial mTORC1 signaling by generating a transgenic mouse overexpressing the rat *Ddit4* gene under the control of a tetracycline reverse transactivator. After intratracheal installation of an adenovirus containing the tet-off tTA-adenovirus (leading to continuous transgene expression in the absence of tetracycline), *Rtp801* transgene expression was apparent via qPCR of lung homogenates (Figure 3A) and via immunofluorescence of lung tissue sections (Figure 3B). The transgene was biologically active, as demonstrated by a decrease in epithelial mTORC1 signaling (Figure 3C) 4 hours after LPS. This loss of mTORC1 activity augmented lung inflammation 24 hours after LPS, as demonstrated by increased BAL neutrophil counts (Figure 3D) and a trend toward worsened histological lung injury scores (Figure 3E). The phenotypes of *Rtp801*^{-/-} and overexpressing Tg-TRE-RTP-801 mice, therefore, consistently demonstrate an anti-inflammatory effect of mTORC1 signaling, with action occurring at least in part through alveolar epithelial cells.

Discussion

Alterations of mTOR signaling participate in disease processes as diverse as obesity and diabetes, cancer growth, and immune dysregulation.¹ However, research into the teleological role of pulmonary mTORC1 as a hub regulating

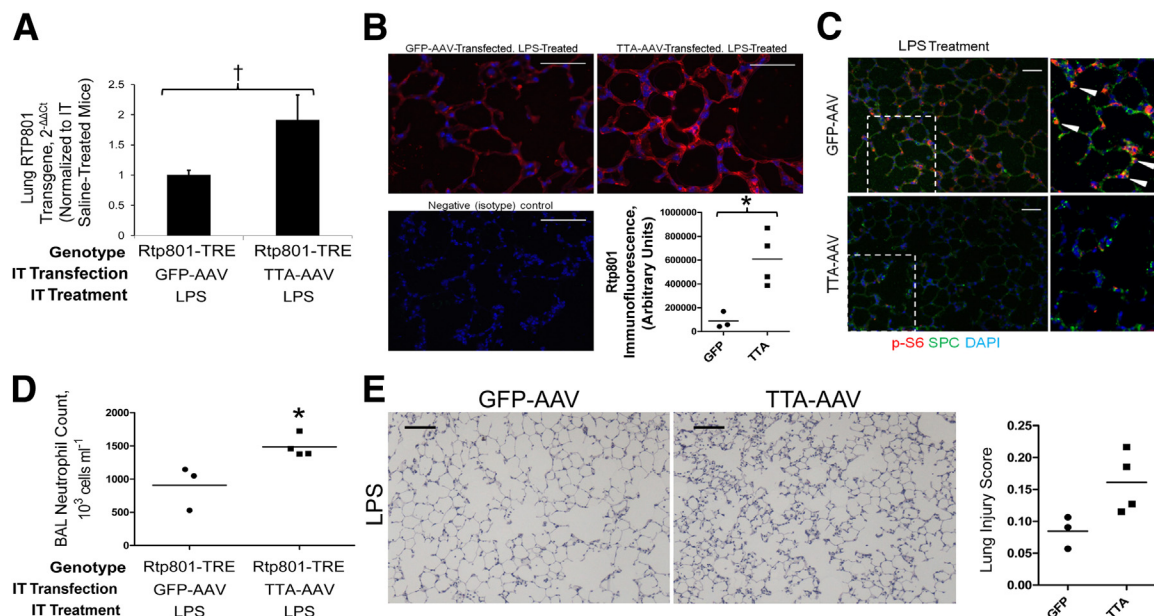


Figure 3 Intratracheal (IT) overexpression of Rtp801 suppresses pulmonary mTORC1 activity and augments LPS-induced lung inflammation. **A:** Intratracheal transfection of Tg-TRE-RTP-801 mice with the tet-off TTA adenovirus increases pulmonary Rtp801 expression by 91% in comparison to Tg-TRE-RTP-801 mice transfected with a GFP-expressing adenoviral control. Expression is quantified as $2^{-\Delta\Delta C_t}$, normalized to both the housekeeping gene cyclophilin A and GFP-AAV-treated controls. **B:** Confirmation of Rtp801 (red) overexpression within alveoli of TTA-AAV-pretreated, LPS-treated Tg-TRE-RTP-801 mice using immunofluorescence. **C:** Transgenic Rtp801 overexpression appropriately functions to suppress mTORC1, as demonstrated by a dramatic attenuation of S6 phosphorylation (p-S6) 4 hours after 2 mg/kg intratracheal LPS. High-magnification inset demonstrates p-S6 colocalization (arrows) with SPC. DAPI = nuclear stain. **D:** Rtp801 overexpression augments pulmonary neutrophilic inflammation, as apparent in BAL 24 hours after 2 mg/kg intratracheal LPS. **E:** These findings are supported by a trend toward increased lung injury in LPS-treated, Rtp801-overexpressing mice. * $P < 0.05$, $^{\dagger}P = 0.05$. $n = 3$ to 4 per group. Scale bars: 50 μm (B and C); 100 μm (E).

environmental stresses and cellular metabolism within the lung has lagged behind other fields of investigation. We have recently identified a key role of epithelial Rtp801/mTOR signaling in the pathogenesis of cigarette smoke–induced pulmonary injury.⁴ We now extend these observations, identifying that induction of Rtp801 importantly contributes to LPS-induced lung inflammation via the suppression of alveolar epithelial mTORC1 signaling.

On the basis of our findings, we propose that alveolar epithelial mTORC1 activity is induced during endotoxin-induced lung injury but is concomitantly attenuated by the induction of endogenous Rtp801. In the absence of Rtp801 suppression, alveolar mTORC1 signaling is significant and attenuates the neutrophil influx characteristic of ARDS. The proinflammatory impact of airway/alveolar Rtp801 overexpression corroborates these findings, further underlining that epithelial mTORC1 signaling attenuates inflammation after intratracheal LPS. In contrast, mTORC1 activity within other alveolar cell types (including inflammatory cells recruited to the injured lung^{7,10}) may have discrepant effects, possibly leading to the variable observations made by us (Figure 2C and previous findings⁴) and others^{7–10} using systemic, pharmacological inhibition of mTORC1 (ie, rapamycin) across the injured alveolar microenvironment.

As a master sensor of environmental stress, mTORC1 is ideally positioned to influence the onset and progression of ARDS, an inflammatory lung disease triggered by direct or indirect environmental stressors. Indeed, mTORC1 regulates numerous processes that directly and indirectly affect lung injury, including apoptosis, oxidative stress, and inflammatory signaling.⁴ Although we were unable to detect a difference in apoptosis between injured WT and *Rtp801*^{−/−} mice, our data demonstrate the broad impact of Rtp801-regulated mTORC1 signaling on oxidative stress (Figure 2D) and inflammation (Figure 2E). In accordance with this proximal role in controlling diverse cellular processes, mTORC1 is highly regulated by a variety of upstream (largely inhibitory) endogenous signaling pathways.¹ Interestingly, these inhibitory pathways impart dramatically different effects on the lung after an inflammatory stimulus. Our observed anti-inflammatory effect of mTORC1 is corroborated by several recent studies. Katholnig et al¹⁶ demonstrated that mTORC1 activation by p38α-MK2 promotes production of the anti-inflammatory cytokine IL-10. Similarly, Ivanov and Roy¹⁷ identified that mTORC1 serves as a translational rheostat, favoring the translation of mRNA encoding anti-inflammatory cytokines (eg, IL-10).

Interestingly, studies of other upstream regulators of mTORC1 activity have not clearly demonstrated an anti-inflammatory effect of mTORC1. AMP-activated protein kinase inhibition of mTORC1 attenuated LPS-induced^{18,19} and bleomycin-induced²⁰ lung injury, whereas it conversely exacerbated wood smoke–induced²¹ and ozone-induced²² lung injury. DEPTOR, an endothelial inhibitor of mTORC1 (as well as extracellular signal–regulated kinase 1/2 and

STAT1 signaling), has been associated with suppression of chemokine and adhesion molecule expression, suggesting anti-inflammatory function.²³

The mechanisms underlying the variable effects of different pathways of mTORC1 inhibition are unclear. Differential tissue expression of various mTORC1 inhibitory pathways could impart varied effects during pulmonary inflammation, indicative of cellular heterogeneity of mTORC1 function within the lung. Our findings, which indicate an epithelial localization of Rtp801/mTORC1 signaling, suggest that alveolar epithelial mTORC1 suppresses pulmonary inflammatory responses to intratracheal LPS. Alternatively, the differing effects of alternative mTORC1 inhibitory pathways could indicate that these pathways impart additional non-specific, mTORC1-independent effects. The reversal of the protective phenotype of *Rtp801*^{−/−} mice by the mTORC1 inhibitor, rapamycin (Figure 2C), reassures us that the observed proinflammatory effects of Rtp801 in our model are mTORC1 dependent.

mTORC1 signaling significantly affects key processes underlying the onset of lung inflammation. The control of this signaling is highly complex, potentially reflecting differential tissue expression of mTORC1 regulatory machinery, such as Rtp801. Future studies with conditional, tissue-specific manipulation of mTORC1 function are needed to further investigate the alveolar heterogeneity of mTORC1 signaling during lung injury.

Acknowledgments

We thank Joel Bowman for assistance in generation of Tg-TRE–RTP-801 mice. The pTetSplice801 flag plasmid used in this study was kindly provided by Quark Pharmaceuticals (Fremont, CA).

References

1. Laplante M, Sabatini D: mTOR signaling in growth control and disease. *Cell* 2012, 149:274–293
2. Ma XM, Blenis J: Molecular mechanisms of mTOR-mediated translational control. *Nat Rev Mol Cell Biol* 2009, 10:307–318
3. Matthay MA, Ware LB, Zimmerman GA: The acute respiratory distress syndrome. *J Clin Invest* 2012, 122:2731–2740
4. Yoshida T, Mett I, Bhunia AK, Bowman J, Perez M, Zhang L, Gandjeva A, Zhen L, Chukwueke U, Mao T, Richter A, Brown E, Ashush H, Notkin N, Gelfand A, Thimmulappa RK, Rangasamy T, Sussan T, Cosgrove G, Mouded M, Shapiro SD, Petrache I, Biswal S, Feinstein E, Tudor RM: Rtp801, a suppressor of mTOR signaling, is an essential mediator of cigarette smoke-induced pulmonary injury and emphysema. *Nat Med* 2010, 16:767–773
5. DeYoung MP, Horak P, Sofer A, Sgroi D, Ellisen LW: Hypoxia regulates TSC1/2-mTOR signaling and tumor suppression through REDD1-mediated 14-3-3 shuttling. *Genes Dev* 2008, 22:239–251
6. Lee DF, Kuo HP, Chen CT, Hsu JM, Chou CK, Wei Y, Sun HL, Li LY, Ping B, Huang WC, He X, Hung JY, Lai CC, Ding Q, Su JL, Yang JY, Sahin AA, Hortobagyi GN, Tsai FJ, Tsai CH, Hung MC: IKK beta suppression of TSC1 links inflammation and tumor angiogenesis via the mTOR pathway. *Cell* 2007, 130:440–455

7. Lorne E, Zhao X, Zmijewski JW, Liu G, Park YJ, Tsuruta Y, Abraham E: Participation of mammalian target of rapamycin complex 1 in Toll-like receptor 2- and 4-induced neutrophil activation and acute lung injury. *Am J Respir Cell Mol Biol* 2009, 41:237–245
8. Fielhaber JA, Carroll SF, Dydensborg AB, Shourian M, Triantafillopoulos A, Harel S, Hussain SN, Bouchard M, Qureshi ST, Kristof AS: Inhibition of mammalian target of rapamycin augments lipopolysaccharide-induced lung injury and apoptosis. *J Immunol* 2012, 188:4535–4542
9. Wang L, Gui YS, Tian XL, Cai BQ, Wang DT, Zhang D, Zhao H, Xu KF: Inactivation of mammalian target of rapamycin (mTOR) by rapamycin in a murine model of lipopolysaccharide-induced acute lung injury. *Chin Med J (Engl)* 2011, 124:3112–3117
10. Nakajima T, Lin KW, Li J, McGee HS, Kwan JM, Perkins DL, Finn PW: T cells and lung injury: impact of rapamycin. *Am J Respir Cell Mol Biol* 2014, 51:294–299
11. Matute-Bello G, Downey G, Moore BB, Groshong SD, Matthay MA, Slutsky AS, Kuebler WM; Acute Lung Injury in Animals Study Group: An official American Thoracic Society workshop report: features and measurements of experimental acute lung injury in animals. *Am J Respir Cell Mol Biol* 2011, 44:725–738
12. Schmidt EP, Yang Y, Janssen WJ, Gandjeva A, Perez MJ, Barthel L, Zemans RL, Bowman JC, Koyanagi DE, Yunt ZX, Smith LP, Cheng SS, Overdier KH, Thompson KR, Geraci MW, Douglas IS, Pearse DB, Tuder RM: The pulmonary endothelial glycocalyx regulates neutrophil adhesion and lung injury during experimental sepsis. *Nat Med* 2012, 18:1217–1223
13. Lygizos MI, Yang Y, Altmann CJ, Okamura K, Hernando AA, Perez MJ, Smith LP, Koyanagi DE, Gandjeva A, Bhargava R, Tuder RM, Faubel S, Schmidt EP: Heparanase mediates renal dysfunction during early sepsis in mice. *Physiol Rep* 2013, 1:e00153
14. Farhangkhoei H, Khan ZA, Mukherjee S, Cukiernik M, Barbin YP, Karmazyn M, Chakrabarti S: Heme oxygenase in diabetes-induced oxidative stress in the heart. *J Mol Cell Cardiol* 2003, 35: 1439–1448
15. Duvigneau JC, Piskernik C, Haindl S, Kloesch B, Hartl RT, Hüttemann M, Lee I, Ebel T, Moldzio R, Gemeiner M, Redl H, Kozlov AV: A novel endotoxin-induced pathway: upregulation of heme oxygenase 1, accumulation of free iron, and free iron-mediated mitochondrial dysfunction. *Lab Invest* 2008, 88:70–77
16. Katholnig K, Kaltenecker CC, Hayakawa H, Rosner M, Lassnig C, Zlabinger GJ, Gaestel M, Muller M, Hengstschlager M, Hörl WH, Park HM, Säemann MD, Weichhart T: p38 α Senses environmental stress to control innate immune responses via mechanistic target of rapamycin. *J Immunol* 2013, 190:1519–1527
17. Ivanov SS, Roy CR: Pathogen signatures activate a ubiquitination pathway that modulates the function of the metabolic checkpoint kinase mTOR. *Nat Immunol* 2013, 14:1219–1288
18. Xing J, Wang Q, Coughlan K, Viollet B, Moriasi C, Zou MH: Inhibition of AMP-activated protein kinase accentuates lipopolysaccharide-induced lung endothelial barrier dysfunction and lung injury in vivo. *Am J Pathol* 2013, 182:1021–1030
19. Zhao X, Zmijewski JW, Lorne E, Liu G, Park YJ, Tsuruta Y, Abraham E: Activation of AMPK attenuates neutrophil proinflammatory activity and decreases the severity of acute lung injury. *Am J Physiol Lung Cell Mol Physiol* 2008, 295:L497–L504
20. Park CS, Bang BR, Kwon HS, Moon KA, Kim TB, Lee KY, Moon HB, Cho YS: Metformin reduces airway inflammation and remodeling via activation of AMP-activated protein kinase. *Biochem Pharmacol* 2012, 84:1660–1670
21. Perng DW, Chang TM, Wang JY, Lee CC, Lu SH, Shyue SK, Lee TS, Kou YR: Inflammatory role of AMP-activated protein kinase signaling in an experimental model of toxic smoke inhalation injury. *Crit Care Med* 2013, 41:120–132
22. Hulo S, Tiesset H, Lancel S, Edmé JL, Viollet B, Sobaszek A, Nevière R: AMP-activated protein kinase deficiency reduces ozone-induced lung injury and oxidative stress in mice. *Respir Res* 2011, 12:64
23. Bruneau SH, Nakayama H, Woda CB, Flynn EA, Briscoe DM: DEPTOR regulates vascular endothelial cell activation and proinflammatory and angiogenic responses. *Blood* 2013, 122:1833–1842